A GLOBAL/LOCAL ANALYSIS METHOD FOR TREATING DETAILS IN STRUCTURAL DESIGN

Mohammad A. Aminpour*

Analytical Services and Materials, Inc.

Susan L. McCleary**

Lockheed Engineering and Sciences Company

Jonathan B. Ransom†

NASA Langley Research Center

525 39

51425

Abstract

A method for analyzing global/local behavior of plate and shell structures is described. In this approach, a detailed finite element model of the local region is incorporated within a coarser global finite element model. The local model need not be nodally compatible (i.e., need not have a one-to-one nodal correspondence) with the global model at their common boundary; therefore, the two models may be constructed independently. The nodal incompatibility of the models is accounted for by introducing appropriate constraint conditions into the potential energy in a hybrid variational formulation. The primary advantage of this method is that the need for transition modeling between global and local models is eliminated. Eliminating transition modeling has two benefits. First, modeling efforts are reduced since tedious and complex transitioning need not be performed. Second, errors due to the mesh distortion, often unavoidable in mesh transitioning, are minimized by avoiding distorted elements beyond what is needed to represent the geometry of the component. The method is applied herein to a plate loaded in tension and transverse bending. The plate has a central hole, and various hole sizes and shapes are studied. The method is also applied to a composite laminated fuselage panel with a crack emanating from a window in the panel. While this method is applied herein to global/local problems, it is also applicable to the coupled analysis of independently modeled components as well as adaptive refinement.

Nomenclature

a minor axis of ellipse
b major axis of ellipse
E Young's modulus

* Research Scientist, 107 Research Drive, Hampton, VA, 23666.

** Senior Engineer, 144 Research Drive, Hampton, VA, 23666.

† Aerospace Engineer, Mail Stop 240, Hampton, VA, 23665.

f generalized force vector
i superscript associated with interface nodes
j subscript associated with subdomains
k subscript associated with interface segment
L length
$\mathbf{K}$ stiffness matrix
K_t stress concentration factor
M_x moment resultant in x-direction
$(M_x)_0$ applied far field moment resultant in x-direction
m number of interface nodes for subdomains
$\mathbf{N}$ generalized displacement shape function matrix
N_x stress resultant in the x-direction
$(N_x)_0$ applied far field stress resultant in x-direction
$\mathbf{n}$ outward unit normal to subdomain interface
n number of pseudo-nodes on interface
o superscript associated with non-interface nodes
p number of degrees of freedom per node
$\mathbf{q}$ generalized displacement vector
$\mathbf{R}$ interpolation matrix for Lagrange multipliers
S interface path
$\mathbf{T}$ interpolation matrix for interface displacements
τ superscript indicating transpose of a matrix
t thickness
$\mathbf{u}$ displacement vector along the interface for subdomains
$\mathbf{v}$ displacement vector on the interface, S
W width
α vector of unknown coefficients for Lagrange multipliers
δ variational operator
λ vector of Lagrange multipliers
ν Poisson's ratio
σ stress tensor
σ_z normal stress component in z-direction
Π total potential energy
Ω domain of discretization

Introduction

The finite element method is the most widely used structural analysis tool mainly due to its flexibility in modeling complicated geometries. While the finite element method can be used to make accurate calculations of detailed stresses, the method is not generally efficient for the design phase because it requires extensive modeling and is computationally expensive. However, with increased utilization of composite materials in aerospace structures, there is a need for detailed modeling at material or geometric discontinuities (e.g., ply dropoffs, cutouts, and stiffener runouts) in order to predict accurately the strength and failure modes of these structures early in the design process. Analytical methods which reduce modeling time while providing the necessary detailed stress and strain states are therefore needed. Global/local analysis is often used to reduce modeling complexities and to predict detailed stress and strain states in structural components.

The global/local analysis of plate and shell structures has, in the past, primarily been accomplished using one of two approaches. The first approach is usually used when the region of interest is not known prior to an analysis[1,2]. In this approach, results from a global analysis are interpolated and applied as boundary conditions on an independent detailed local model. While this approach leads to a smaller overall problem size and simplified modeling, methods developed using the approach usually provide no interaction between the local and global models. To overcome this problem, an iterative global/local method[3] has recently been proposed that provides for this interaction. This method, however, has been applied only to mesh discretizations with a one-to-one nodal correspondence across the boundary between subdomains. Finite element meshes which preserve this one-to-one nodal correspondence across the boundary between subdomains will hereafter be referred to as nodally compatible.

The second approach, usually used when the region of interest is known *a priori*, typically involves a single finite element analysis with the finite element mesh highly refined in the known region of interest[4-6]. This approach may, however, lead to highly complex modeling because mesh transitioning between the local region and the rest of the model is essential to obtain a solution to the problem in a timely and cost effective manner.

Recently, a third approach, which combines the desirable features of the first two approaches, has been the subject of research. The methods developed using this approach provide modeling flexibility (i.e., they permit independent modeling of global and local subdomains) as well as a coupling of the global and local analyses (i.e., they provide the necessary interaction between the global and local models). Some of these methods have concentrated on the development of techniques for parallel computers[7-8] while others have used some form of multi-point constraints along the common subdomain boundaries[9-10]. In reference 11, three formulations for coupling the independently modeled regions were developed and studied. The hybrid variational formulation was shown to be the most robust and accurate of the three examined.

The purpose of this paper is to describe a coupled global/local analysis method developed using the third approach. This method couples global and local subdomains using an independent function along the interface between the subdomains[11]. The nodal compatibility of the models is accounted for by introducing appropriate constraint conditions into the total potential energy functional.

The description of the coupled global/local analysis method is presented, followed by two applications of the method to plate and shell structures. The first application is a plate loaded in tension and transverse bending. The plate has a central hole, and various hole sizes and shapes are studied. In these analyses, the region in the vicinity of the hole is taken to be the local region; the remainder of the panel is taken to be the global region, and the two regions are modeled independently. The second application is a composite laminated fuselage panel with a crack emanating from a window in the panel. In this analysis, the region in the immediate vicinity of the crack is taken to be the local region and

the remainder of the panel is taken to be the global region. While these demonstration problems are typical global/local problems, the present coupled analysis method is also applicable to the analysis of independently modeled components and may be used to perform adaptive refinement.

Description of Coupled Global/Local Analysis Method

The coupled analysis method presented herein allows the independent modeling of different regions or components without concern for the nodal compatibility between the finite element models. Transition modeling between a region with a fine mesh and a region with a coarse mesh is no longer necessary. This approach prevents changes in the modeling of the local region from affecting the modeling in the global region. For example, with a judiciously chosen local model, an analyst may perform a geometrically parametric study of hole size and shape by changing the mesh in the immediate vicinity of the hole, without having to change the modeling of the global region.

This method does not improve the performance of the finite elements used in the analysis and therefore does not improve the quality of the results attainable by a particular element. However, by eliminating or reducing transition modeling, the introduction of distorted elements into the finite element model is limited to what is necessary to represent the geometry of the component. Therefore, no additional errors associated with mesh distortion are introduced. The elimination of unnecessary element distortion errors allows the use of coarser meshes, and, therefore, the same qualitative results may be obtained with a smaller number of degrees of freedom.

The method described herein may generally be applied to connect an arbitrary number of independently modeled subdomains. However, in the following discussion, the mathematical formulation will be described in terms of two subdomains and a single, multi-segmented interface. Consider a two-dimensional domain, Ω, that is modeled as two independently discretized subdomains, Ω_1 and Ω_2, as shown in Figure 1. The interface, S, is modeled as two semi-independent line segments. Each segment of the interface, S, is discretized with evenly spaced "pseudo-nodes" (open circles in Figure 1) which need not conform to the discretization of either of the subdomains. An interface such as that shown in Figure 1 is considered to be a single, two-segmented interface (segments AB and BC in Figure 1). At the corner (point B in Figure 1), a pseudo-node must exist.

The displacement vector along each interface segment, k, may be written as

$$\mathbf{v} = \mathbf{T}\mathbf{q}, \tag{1}$$

where $\mathbf{T}$ is a $p \times pn_k$ matrix of interpolating functions, and $\mathbf{q}_s$ is a vector of pn_k generalized displacements associated with the n_k interface pseudo-nodes each having p degrees of freedom. The specific form of the matrix $\mathbf{T}$ depends on the type of function chosen and the number of evenly spaced pseudo-nodes, n_k, selected along segment k of the interface, S. As in reference 11, cubic splines are used to describe the

970

displacement field vector, v, along each segment of the interface, S. Equation 1 is assumed to be valid along each segment (segments AB and BC in Figure 1); at the interface corner (point B in Figure 1), the values from each interface segment are constrained to be the same.

In the hybrid variational formulation, the total potential energy equation is modified to include an integral form for the compatibility between the interface and the subdomains and is given by

$$\Pi = \Pi_{\Omega_1} + \Pi_{\Omega_2} + \int_S \lambda_1^T (v - u_1)\, ds + \int_S \lambda_2^T (v - u_2)\, ds \tag{2}$$

where Π_{Ω_j} is the total potential energy, λ_j is a vector of Lagrange multipliers, and u_j is the displacement field vector along the interface for subdomain j. The constraint integrals are added to the functional to enforce the continuity, in the variational sense, of displacements across the interface. Equation 2 corresponds to the "double layer interface" or "frame" method of the hybrid variational principle[12] and has in the past been used primarily to enforce compatibility between adjacent elements that have incompatible assumed displacement shape functions within the context of a nodally compatible finite element model[13–16]. Herein, however, the variational statement in equation 2 is utilized to enforce compatibility between nodally incompatible finite element models.

Assuming that the displacement boundary conditions are satisfied, the stationary condition for the modified total potential energy for arbitrary u_j in the subdomains, arbitrary v on the interface, S, and arbitrary λ_j on the interface parts of the subdomains, results in the following Euler equations

$$\delta\Pi = 0 \quad \Rightarrow \quad \begin{cases} \lambda_j = (\sigma n)_j\,; & j = 1, 2 \\ \lambda_1 + \lambda_2 = 0 & \\ u_j = v; & j = 1, 2 \end{cases} \quad \text{on } S. \tag{3}$$

These equations are in addition to the usual Euler equations which satisfy the equilibrium equations and traction boundary conditions. In equation 3, σ is the stress tensor and n is the outward unit normal to the subdomain interface. Thus, equation 3 states that λ_j represent the tractions on the interface for subdomain j and that the sum of the tractions across the interface is zero (i.e., equilibrium is maintained, in the variational sense, across the interface). Equation 3 also states that the displacement field on the interface for subdomain j is equal to the assumed displacement field, v, along the interface (i.e., displacement continuity is maintained, in the variational sense, across the interface).

In the finite element discretization, the displacements, u_j, and the Lagrange multipliers, λ_j, are independently approximated for each element along the interface, and the displacement field, v, is approximated on the interface, S, as discussed previously. The displacements, u_j, along the interface are expressed in terms of unknown nodal displacements, q_j^i, as $u_j = N_j q_j^i$, and the Lagrange multipliers, λ_j, are expressed in terms of unknown coefficients, α_j, as $\lambda_j = R_j \alpha_j$, where N_j and R_j are matrices of interpolating functions. The interpolating functions in the matrix, R_j, are taken to be constant parameters for linear elements and linear functions for quadratic elements. With these assumptions,

equation 2 may be rewritten as

$$\Pi = \Pi_{\Omega_1} + \Pi_{\Omega_2} + \alpha_1^T M_1^T q_1^i + \alpha_2^T M_2^T q_2^i + \alpha_1^T G_1^T q_s + \alpha_2^T G_2^T q_s \tag{4}$$

where M_j and G_j are integrals on the interface defined in terms of R_j, N_j, and T as

$$M_j = -\int_S N_j^T R_j ds \quad \text{and} \quad G_j = \int_S T^T R_j ds \quad ; \quad j = 1, 2 \tag{5}$$

Taking the first variation of the modified total potential energy with respect to the independent variables $(q_j^i, q_j^o, q_s, \alpha_j, j = 1, 2)$ and setting it to zero yields the system of equations

$$
\begin{bmatrix}
K_1^{ii} & K_1^{io} & 0 & 0 & 0 & M_1 & 0 \\
K_1^{oi} & K_1^{oo} & 0 & 0 & 0 & 0 & 0 \\
0 & 0 & K_2^{ii} & K_2^{io} & 0 & 0 & M_2 \\
0 & 0 & K_2^{oi} & K_2^{oo} & 0 & 0 & 0 \\
0 & 0 & 0 & 0 & 0 & G_1 & G_2 \\
M_1^T & 0 & 0 & 0 & G_1^T & 0 & 0 \\
0 & 0 & M_2^T & 0 & G_2^T & 0 & 0
\end{bmatrix}
\begin{bmatrix}
q_1^i \\ q_1^o \\ q_2^i \\ q_2^o \\ q_s \\ \alpha_1 \\ \alpha_2
\end{bmatrix}
=
\begin{bmatrix}
f_1^i \\ f_1^o \\ f_2^i \\ f_2^o \\ 0 \\ 0 \\ 0
\end{bmatrix}
\tag{6}
$$

where q_j is the generalized displacement vector, f_j is the external force vector, and K_j is the stiffness matrix associated with subdomain j. The system of equations given by equation 6 is symmetric, not banded and not positive definite. Thus, a general solver which uses Gaussian elimination and operates on a dense matrix is used in this case. Therefore, modeling efficiency has been achieved at the expense of possible additional computer time required to solve the system of equations. The above system of equations may also be partially solved first (e.g., using a singular value decomposition algorithm two times) to obtain a smaller, symmetric, and positive definite system of equations which may be solved by conventional solvers. It is also believed that current and future fast parallel and serial computers and new solution algorithms will address the problem of computational efficiency and that this problem should not be considered a serious drawback for the present method described herein.

Applications

The coupled analysis approach described in this paper and validated in reference 11 has been utilized to analyze representative global/local examples. An isotropic plate subjected to tension and transverse bending is first analyzed. The plate has a central hole, and various hole shapes and sizes are studied. This example demonstrates the use of the coupled analysis method in studying the effect of details in structural design, such as hole configuration. The effectiveness of the method is then demonstrated on a more complicated example. In this example, a representative composite laminate fuselage panel with simulated stringers and frames and with a crack emanating from a window in the panel is analyzed. A nine-node assumed natural-coordinate strain (ANS) element[17] is used in the problems discussed in this paper. This element has five degrees of freedom at each node (i.e., three displacements and two bending rotations) and uses a strain field approximation (equivalent to a selective directionally reduced order of integration) to calculate the element stiffness matrix.

972

Plate with a Central Hole

An isotropic plate with a central hole (shown in Figure 2) is an ideal structure to verify the global/local capability of the method since solutions are available in the literature. In addition, geometrically parametric studies may be performed to demonstrate the added modeling flexibility provided by the method. Tension and transverse bending loads are applied to the plate, and various hole sizes and shapes are studied.

Taking advantage of symmetry, only a quarter of the plate is modeled in the coupled analysis. The region in the vicinity of the hole is taken to be the local region and the remainder is taken to be the global region. The hole size and shape are varied by changing the finite element model of the local region, while the model of the global region remains unchanged. The finite element meshes for the global model and four typical local models with different hole configurations are shown in Figure 3.

The stress concentration factor, K_t, for an infinite plate in tension which has a central circular hole is defined as the ratio of the maximum longitudinal stress resultant, $(\mathbf{N}_x)_{max}$, to the far field longitudinal stress resultant, $(\mathbf{N}_x)_0$. The exact value of K_t is 3 for an infinite isotropic plate[18]. For a finite-width plate loaded in tension with a half-width, w, and with a central circular hole of radius a the stress concentration factor, K_t, may be defined as the ratio of the maximum longitudinal stress resultant, $(\mathbf{N}_x)_{max}$, to the nominal longitudinal stress resultant, $(\mathbf{N}_x)_{nom}$, where

$$(\mathbf{N}_x)_{nom} = \frac{(\mathbf{N}_x)_0}{(1 - \frac{a}{w})}$$

The finite-width effects on the stress concentration factors for an isotropic plate loaded in tension and having a circular hole have been obtained numerically by Howland[19], using successive approximations, and reproduced by Peterson[20]. Figure 4 shows the stress concentration factor as a function of the hole radius to plate half-width ratio, $\frac{a}{w}$. The coupled analysis solution is seen to be in excellent agreement with the solution by Howland.

The stress concentration factor, K_t, for an infinite plate subjected to transverse bending and having a central circular hole is defined as the ratio of the maximum longitudinal moment resultant, $(M_x)_{max}$, to the far field longitudinal moment resultant, $(M_x)_0$. The exact solution for the stress concentration factor for an infinite plate subjected to transverse bending and having a circular hole has been obtained by Goodier[21] and Reissner[22] and reproduced by Peterson[20]. The exact solution for the stress concentration factor along with the results obtained by the coupled method are shown in Figure 5 as a function of the hole diameter to plate thickness ratio, $\frac{2a}{t}$. The coupled analysis solution is in excellent agreement with the exact solution.

The effect of the hole shape on the stress concentration factor for an infinite plate subjected to tension and transverse bending is shown in Figures 6 and 7, respectively. The exact solution for the

stress concentration factor for an infinite plate subjected to tension load has been obtained by Kolosoff[23] and Inglis[24], and reproduced by Peterson[20]. The stress concentration factor for an infinite plate subjected to a pure transverse bending load has been obtained by Goodier[21] and reproduced by Peterson[20]. The stress concentration factor for each load case is shown as a function of the ratio of the hole axes, $\frac{a}{b}$. The coupled analysis is in excellent agreement with the exact solution for each loading condition.

Composite Fuselage Panel

In the second application, the coupled analysis method is applied to a composite fuselage panel shown in Figure 8. It should be emphasized that the purpose of this example is not to perform a comprehensive detailed analysis of a complicated panel, but rather to demonstrate that the method described herein may be utilized to perform such analyses. The panel is made of a 16 ply composite laminate $(\pm 45/0_2/\pm 45/90_2)_s$. Stringer and frame actions are simulated by constraining appropriate motions of the panel along the stringer and frame paths as shown in Figure 8. A hole is introduced at the center of the panel to simulate a window. The square window has rounded corners, and there is a crack emanating from one of the corners. The loading on this panel is composed of a uniform pressure load on the concave side of the panel and uniform displacements applied on the curved edges of the panel in the longitudinal direction in order to simulate typical loads experienced by a panel in a fuselage under hydrostatic pressure. To simulate the presence of glass in the window, an equivalent approximate load is applied to the edges of the hole. This load is calculated by integrating the constant pressure over the surface of the window and distributing the result uniformly around the edge of the hole. The region in the immediate vicinity of the crack is taken to be the local region. The rest of the panel is taken to be the global region, and the two regions are modeled independently (see Figure 9). For this example, the interface between the local and global regions has a slightly curved geometry (which is due to the curvature of the panel) and is composed of four segments (which are shown as four straight line segments in Figure 9c forming the boundaries of the local model). The model for the coupled analysis has 4591 active degrees of freedom.

Since there are no theoretical solutions for this example, a reference solution is obtained using a finite element model of the panel (shown in Figure 10) which does not have an interface. This finite element model has the same refinement in the region around the crack-tip as the local model used in the coupled analysis. In order to avoid transition modeling, this high level of discretization is extended around the entire hole. The reference solution model is also more refined in the region away from the window than the global model used in the coupled analysis due to the propagation of the local discretization. The model for the reference solution has 11876 active degrees of freedom, which is nearly 2.6 times as many degrees of freedom as the model in the coupled analysis. Although there are many ways to model this panel, (e.g., the region around the hole and away from the crack-tip need not be

as fine in the reference model), this reference model was selected because of ease of modeling and to minimize transition modeling.

The deformation patterns for global/local analysis and the reference solution are shown in Figure 11. The distribution of axial stress, σ_z, from the coupled analysis and the reference solution are shown in Figure 12. A comparison of the results shown in Figures 11 and 12 reveals that the coupled analysis correlates well with the reference solution. In fact, the maximum value of the normal displacement obtained from the coupled analysis is within 0.08% of the reference solution. Moreover, the maximum value of the stresses obtained from the coupled analysis is within 1% of the reference solution. Therefore, quantities such as stress intensity factors and the strain energy release rates will also be nearly identical. Thus, one may obtain quantities such as critical crack length (which indicates the onset of unstable crack growth) by incrementally extending the crack length and repeating the coupled analysis until the critical stress intensity factors and critical strain energy release rates are obtained. A comparison of the stress distribution between the coupled analysis and the reference solution demonstrates the robustness of the method.

Concluding Remarks

A coupled analysis method for analyzing plate and shell structures composed of two or more independently modeled finite element subdomains has been described and applied herein to selected global/local examples. The method allows the analyst to incorporate a detailed model of the local subdomain within the global model. The local model need not be nodally compatible with the global model. Thus, the need for tedious transition modeling is eliminated. A hybrid variational formulation was utilized to achieve compatibility, in a variational sense, between the nodally incompatible models.

The coupled analysis method described herein was applied to two demonstration problems: (1) an isotropic plate which is loaded in tension and transverse bending and which has a central hole of various sizes and shapes, and (2) a composite fuselage panel with a crack emanating from a window cutout. Excellent agreement was obtained between the coupled analysis solutions and the reference solutions in each case. The capability of the method for treating details in structural design was demonstrated by the parametric study of the hole configuration in the isotropic plate example. The potential of the method for the detailed analysis of complicated shell structures was demonstrated by the coupled analysis of a composite fuselage panel with a crack emanating from a window cutout.

The coupled analysis method presented herein provides a technique for predicting local, detailed stress states for plate and shell structures. The simplified modeling provided by the coupled analysis method should enhance efficiency of analysis methods and provide the modeling flexibility needed to address local details. Such enhancements should lead to a means of integrating detailed analysis into the design process.

References

1. Jara-Almonte, C.C., and Knight, C .E., "The Specified Boundary Stiffness/Force SBSF Method for Finite Element Subregion Analysis," *International Journal for Numerical Methods in Engineering*, Vol. 26, 1988, pp. 1567-1578.

2. Ransom, J.B., and Knight, N.F., Jr., "Global/Local Stress Analysis of Composite Panels," *Computers and Structures*, Vol. 37, No. 4, 1990, pp. 375-395.

3. Whitcomb, J.D., "Iterative Global/Local Finite Element Analysis," *Computers and Structures*, Vol. 40, No. 4, 1991, pp. 1027-1031.

4. Hirai, I., Wang, B. P., and Pilkey, W. D., "An Efficient Zooming Method for Finite Element Analysis," *International Journal for Numerical Methods in Engineering*, Vol. 20, 1984, pp. 1671-1683.

5. Hirai, I., Wang, B. P., and Pilkey, W. D., "An Exact Zooming Method," *Finite Element Analysis and Design*, Vol. 1, No. 1, April 1985, pp. 61-68.

6. *ANSYS User's Manual*, Swanson Analysis Systems, Inc., Houston, PA, 1979.

7. Farhat, C., "A Method of Finite Element Tearing and Interconnecting and its Parallel Solution Algorithm," *International Journal for Numerical Methods in Engineering*, Vol. 32, No. 6, 1991, pp. 1205-1228.

8. Maday, Y., Mavriplis, D., and Patera, A., "Nonconforming Mortar Element Methods: Application to Spectral Discretizations," NASA CR-181729, ICASE Report No. 88-59, October 1988.

9. Shaeffer, H.G., *MSC/NASTRAN Primer, Static and Normal Modes Analysis*, Shaeffer Analysis, Inc., Mont Vernon, New Hampshire 1979, pp. 262-265.

10. Krishnamurthy, T., and Raju, I. S., "An Independent Refinement and Integration Procedure in Multiregion Finite Element Analysis," *Proceedings of the 33rd AIAA/ASME/ASCE/AHS/ASC Structures, Structural Dynamics and Materials Conference*, Part 1, April 13-15, 1992, Dallas, TX, pp. 302-312.

11. Aminpour, M.A., Ransom, J.B., and McCleary, S.L., "Coupled Analysis of Independently Modeled Finite Element Subdomains," *Proceedings of the 33rd AIAA/ASME/ASCE/AHS/ASC*

Structures, Structural Dynamics and Materials Conference, Part 1, April 13-15, 1992, Dallas, TX, pp. 109-120.

12. Zienkiewicz, O.C., *The Finite Element Method*. Third Edition, McGraw–Hill Book Company, UK, 1977, pp. 304-328.

13. Atluri, S.N., Nishioka, T., and Nakagaki, M., "Numerical Modeling of Dynamic and Nonlinear Crack Propagation in Finite Bodies by Moving Singular Elements," *Nonlinear and Dynamic Fracture Mechanics*, (Edited by N. Perrone and S.N. Atluri, AMD), Vol. 35, ASME 1979, pp. 37-66.

14. Gunther, C.K., Holsapple, K.A., and Kobayashi, A.S., "Finite Element Analysis of Cracking Bodies," *AIAA J.* 19, 1981, pp. 789-795.

15. Aminpour, M.A., and Holsapple, K.A., "Finite Element Solutions for Propagating Interface Cracks with Singularity Elements," *Engineering Fracture Mechanics*, Vol. 39, No. 3, 1991, pp. 451-468.

16. Jinping, Z., and Huizu, S., "Stress Analysis Around Holes in Orthotropic Plates by the Subregion Mixed Finite Element Method," *Computers and Structures*, Vol. 41, No. 1, 1991, pp. 105-108.

17. Park, K.C.; Stanley, G.M., "A Curved C^0 Shell Element Based on Assumed Natural-Coordinate Strains," *ASME Journal of Applied Mechanics*, Vol. 108, 1986, 278–290.

18. Timoshenko, S.P., and Goodier, J.N., *Theory of Elasticity*. Third Edition, McGraw-Hill Book Company, New York, 1970, pp. 90-97.

19. Howland, R.C., "On the Stresses in the Neighborhood of a Circular Hole in a Strip under Tension," *Phil. Trans. Roy. Soc.* (London) A, Vol. 229, 1929-30.

20. Peterson, R.E., *Stress Concentration Design Factors*, Wiley-International, New York, 1953.

21. Goodier, J.N., "Influence of Circular and Elliptical Holes on Transverse Flexture of Elastic Plates," *Phil. Mag.*, Vol. 22, 1936.

22. Reissner, E., "The Effect of Transverse Shear Deformation on the Bending of Elastic Plates," *Trans. ASME*, Vol. 67, 1945.

23. Kolosoff, G., Dissertation, St. Petersburg, 1910.

24. Inglis, C.E., "Stresses in a Plate due to the Presence of Cracks and Sharp Corners," *Engineering* (London), Vol. 95, 1913.
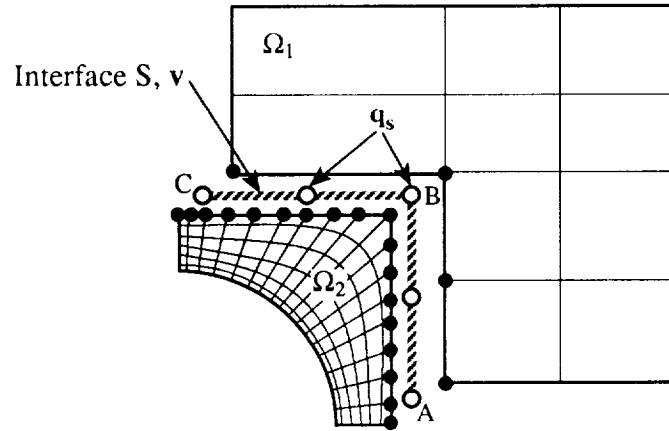
Figure 1. Interface definition for coupled analysis

$L/w = 2$ $0.0083 \leq a/w \leq 0.3$
$\nu = 1/3$ $1/6 \leq a/b \leq 6.0$
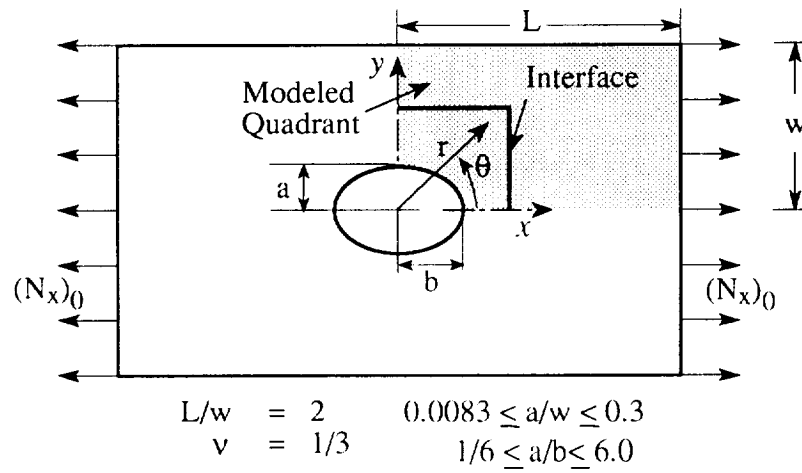
Figure 2. Plate with central hole
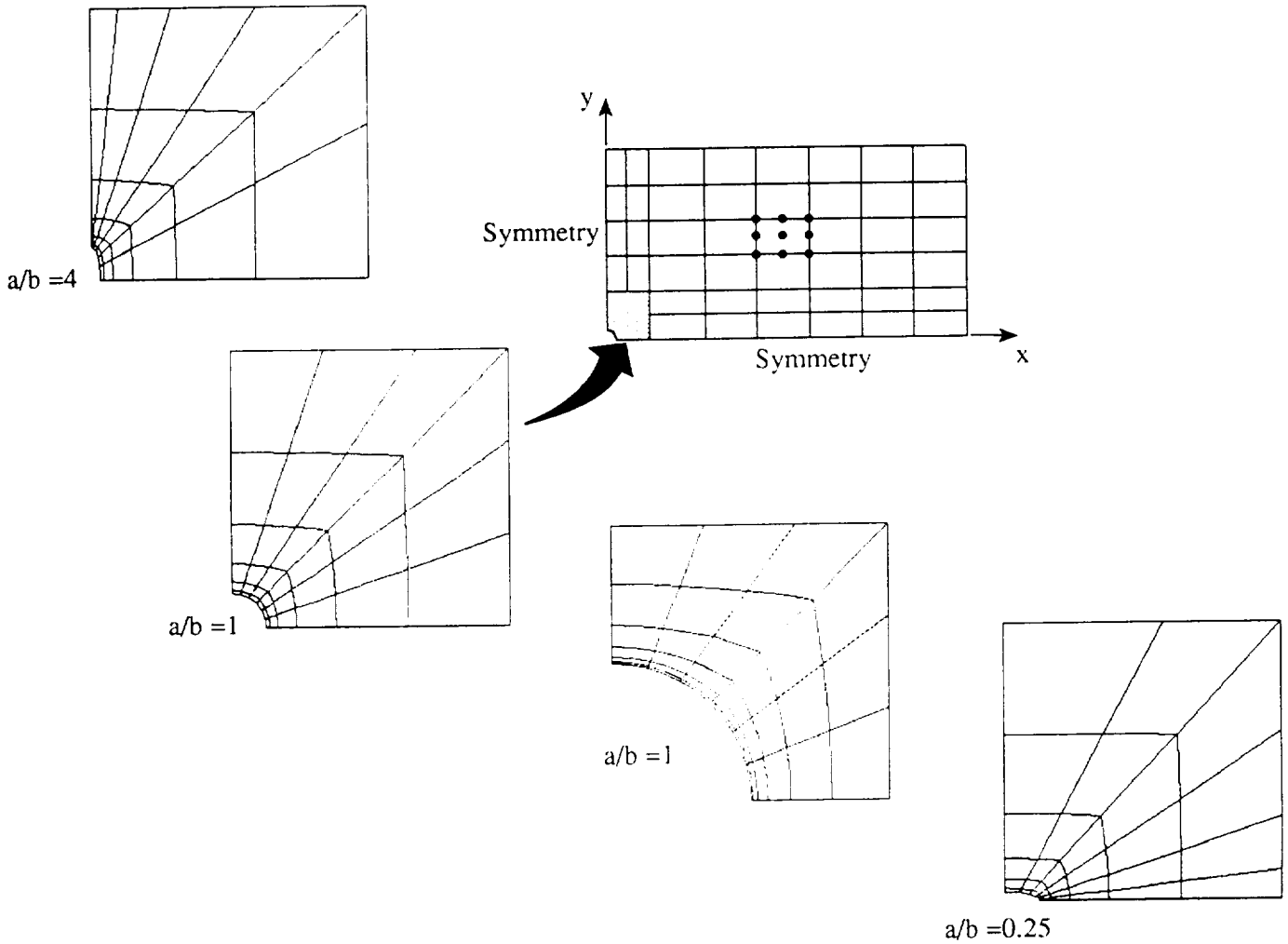
Figure 3. Finite element models for local and global regions of plate with hole
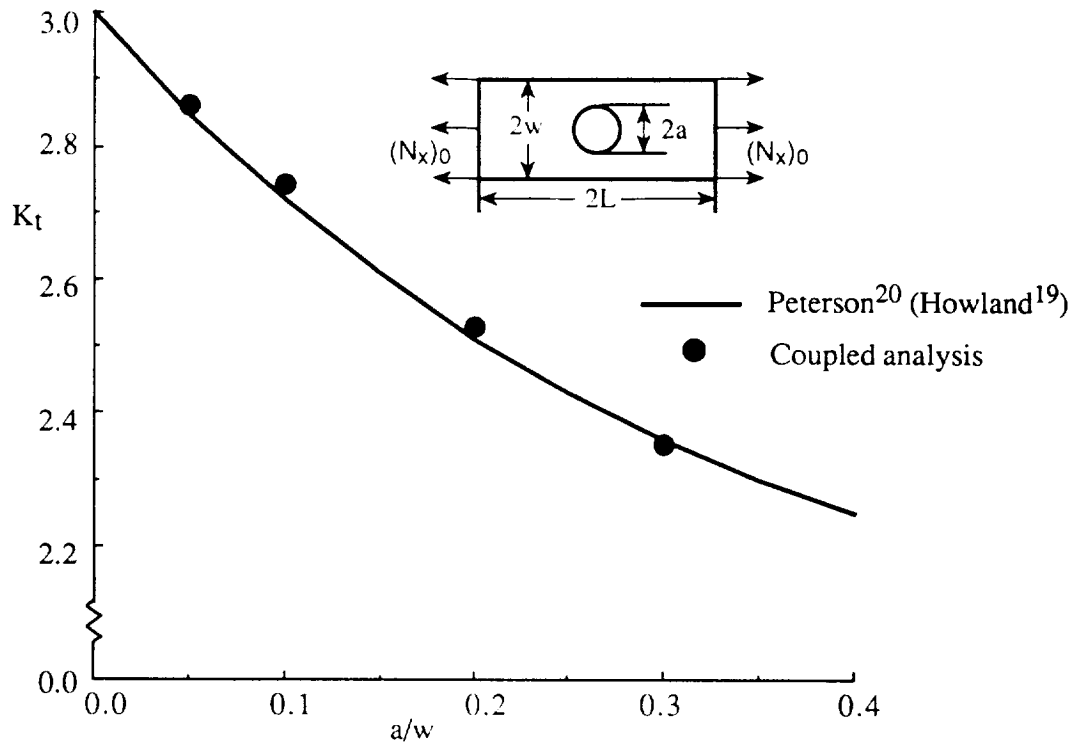
Figure 4. Stress concentration factor, K_t, of finite-width plate subjected to inplane tension
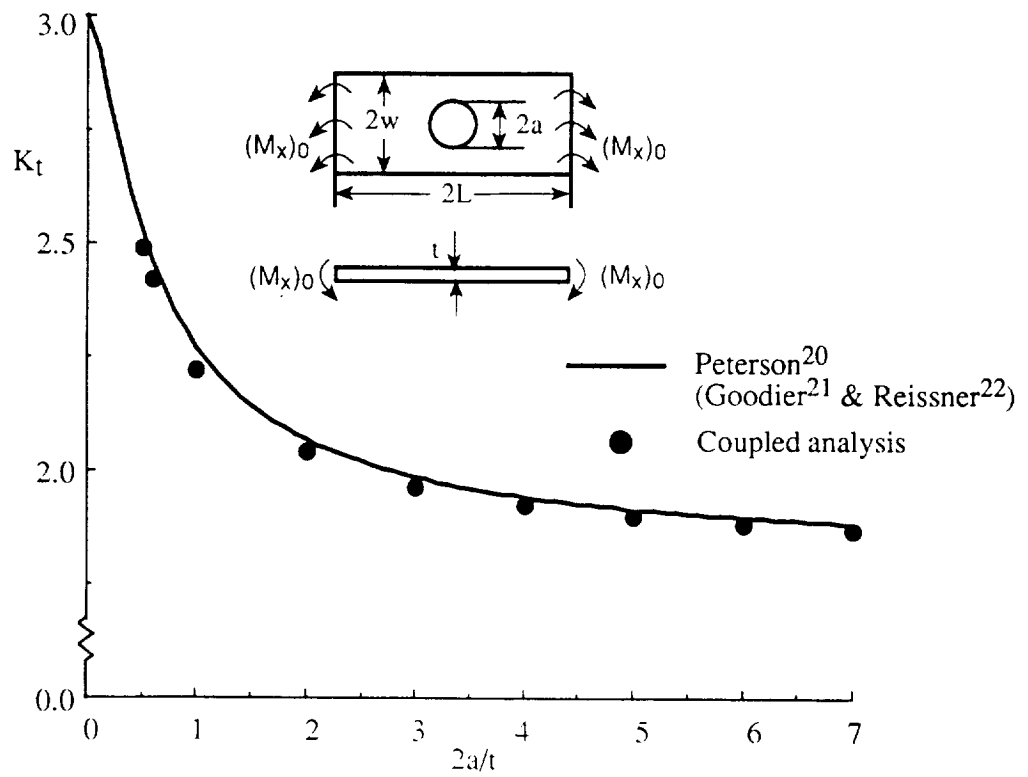

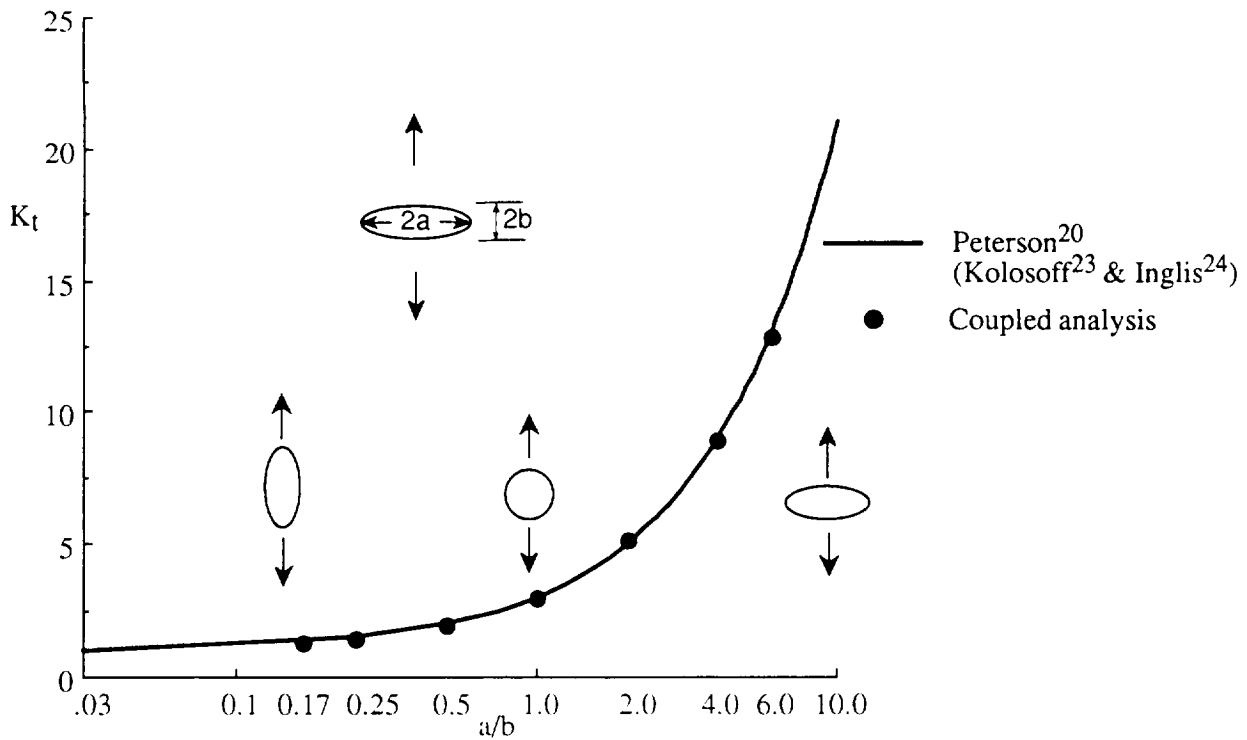Figure 5. Stress concentration factor, K_t, of infinite plate subjected to transverse bending

Figure 6.   Effect of hole configuration on stress concentration factor, K_t, of infinite plate subjected to inplane tension
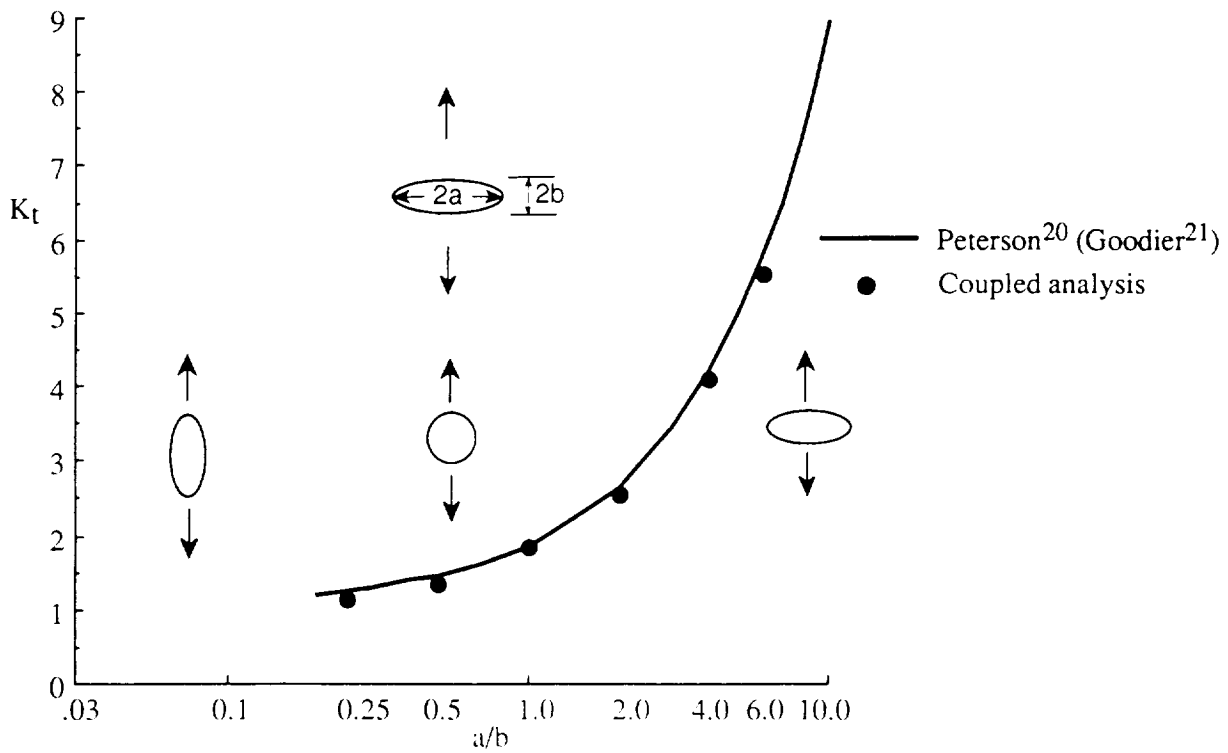
Figure 7.   Effect of hole configuration on stress concentration factor, K_t, of infinite plate subjected to transverse bending
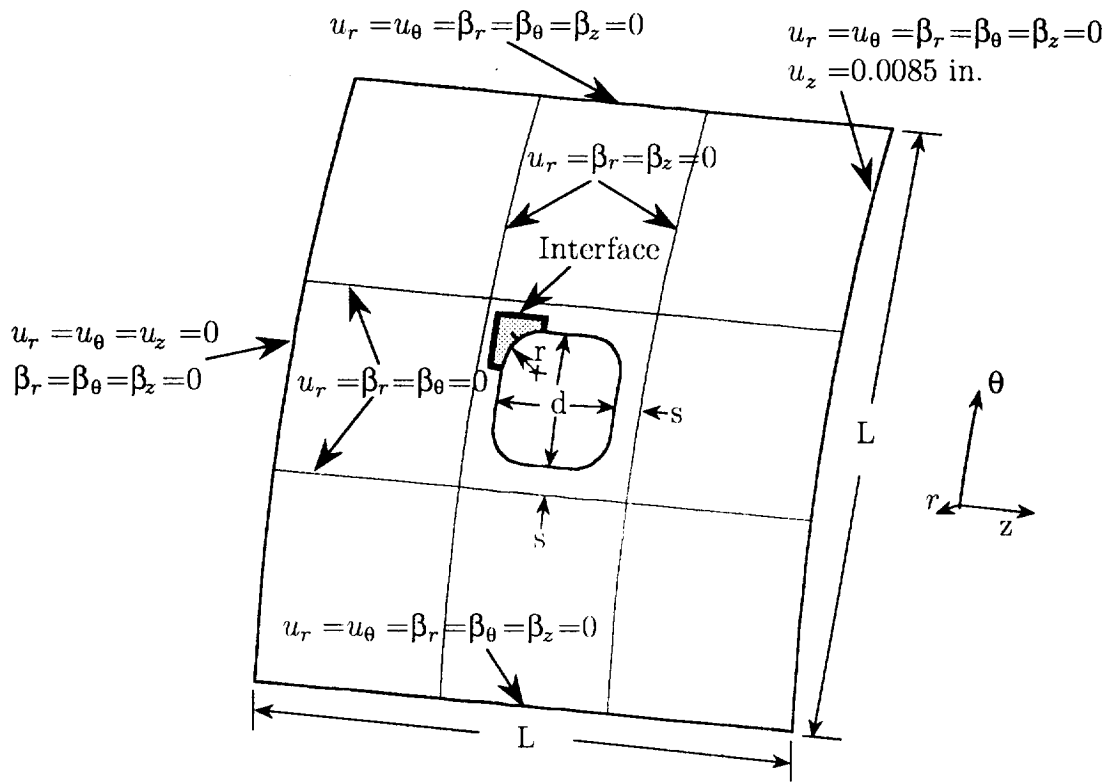
$$E_1 = 18500 \text{ ksi} \qquad s = 1.5 \text{ in.}$$
$$E_2 = 1890 \text{ ksi} \qquad d = 7.0 \text{ in.}$$
$$V_{12} = 0.38 \qquad r = 2.0 \text{ in.}$$
$$t_{ply} = 0.0056 \text{ in.} \qquad L = 32.0 \text{ in.}$$
$$t_{lam} = 0.3136 \text{ in.} \qquad R = 85.0 \text{ in (panel radius)}$$
$$p = 10.0 \text{ psi} \qquad \text{panel arc is } 21.6 \text{ degrees}$$

Figure 8. Cracked fuselage panel
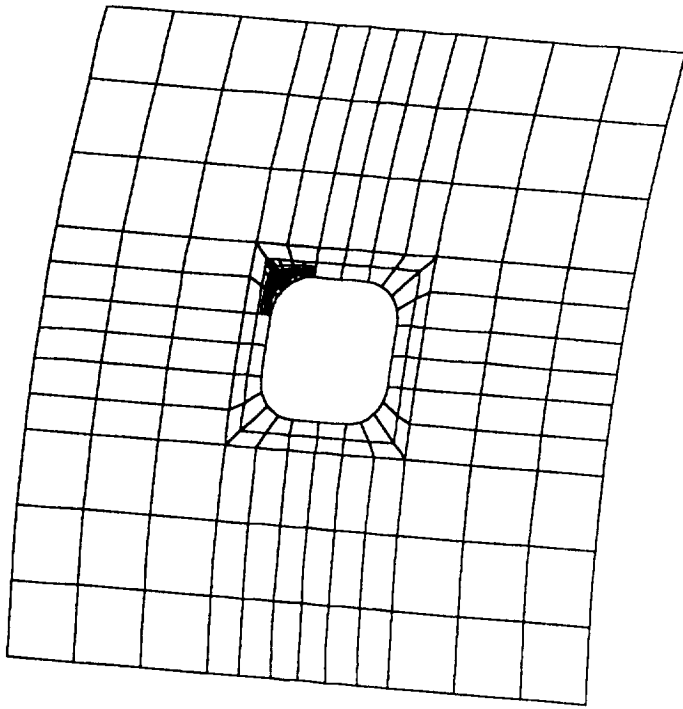
a. Global model
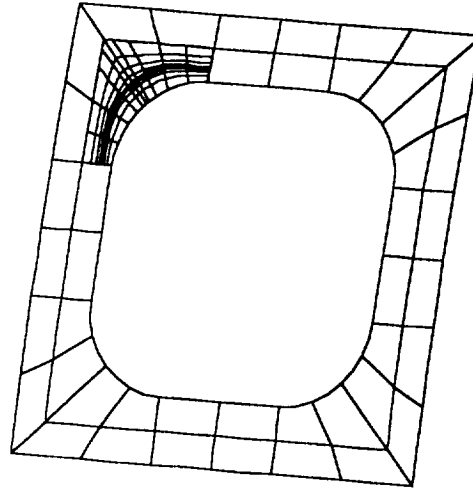
b. Close-up of region around hole
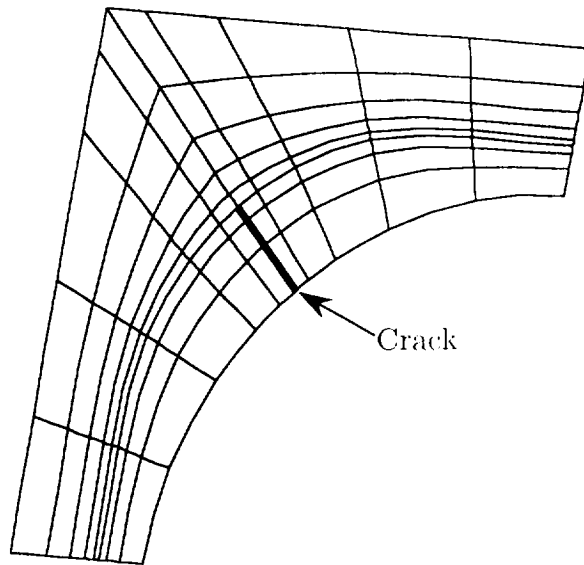
c. Local Model

Figure 9. Finite element models for coupled analysis
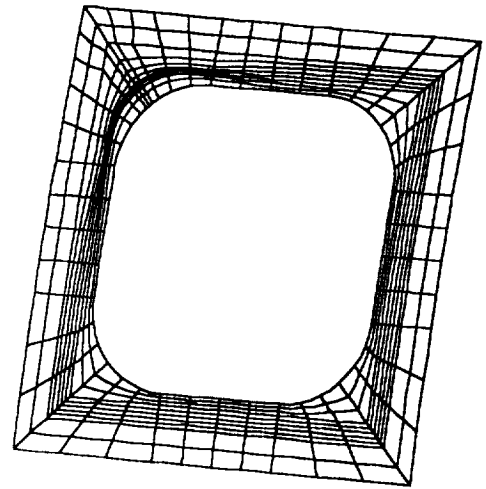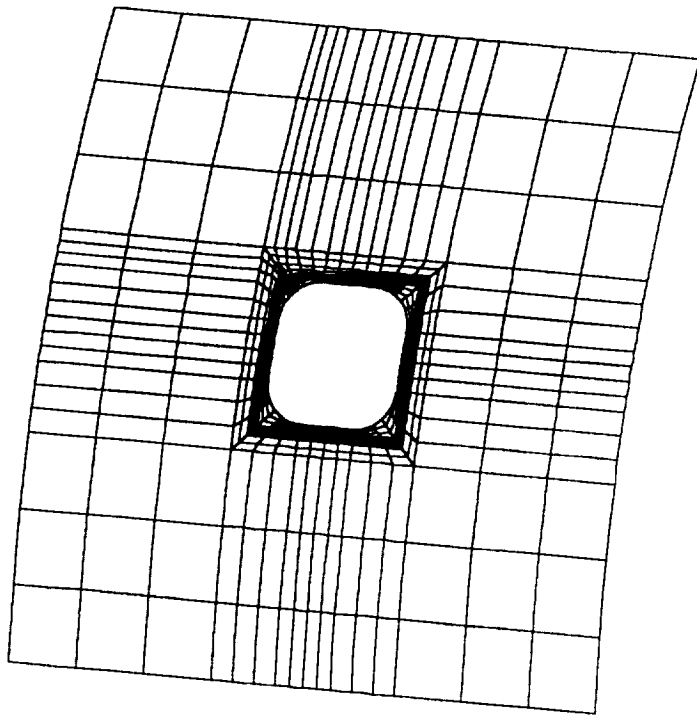
Close-up of region around hole

Figure 10. Finite element model for reference solution
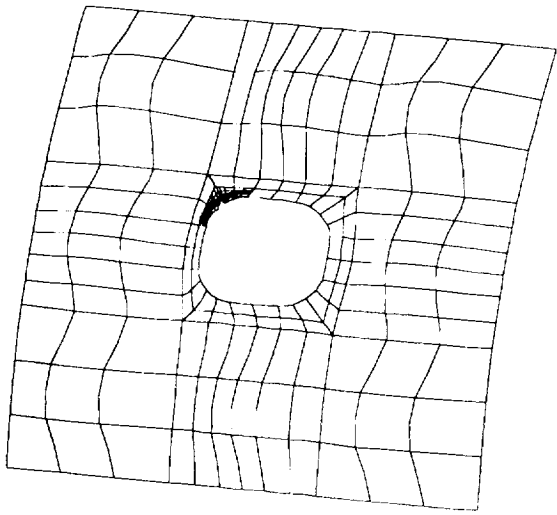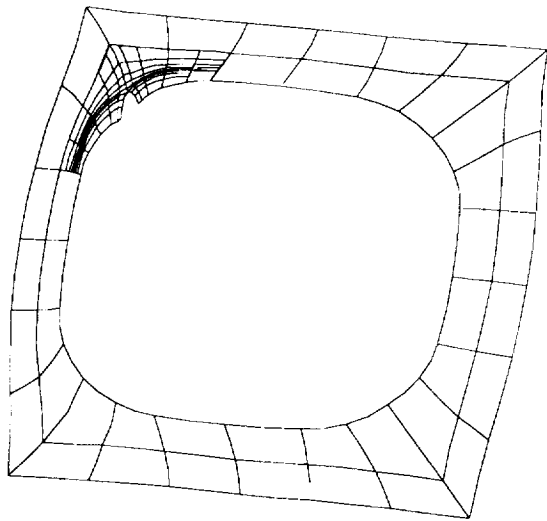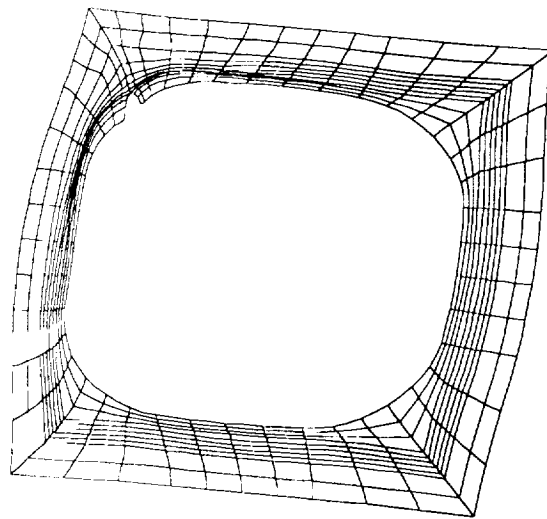
Coupled analysis solution   Reference solution
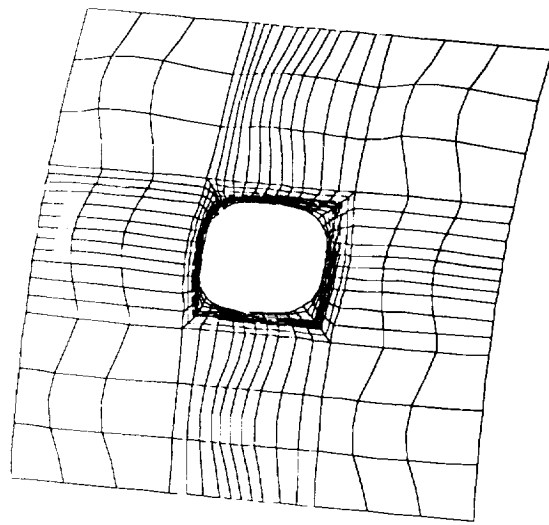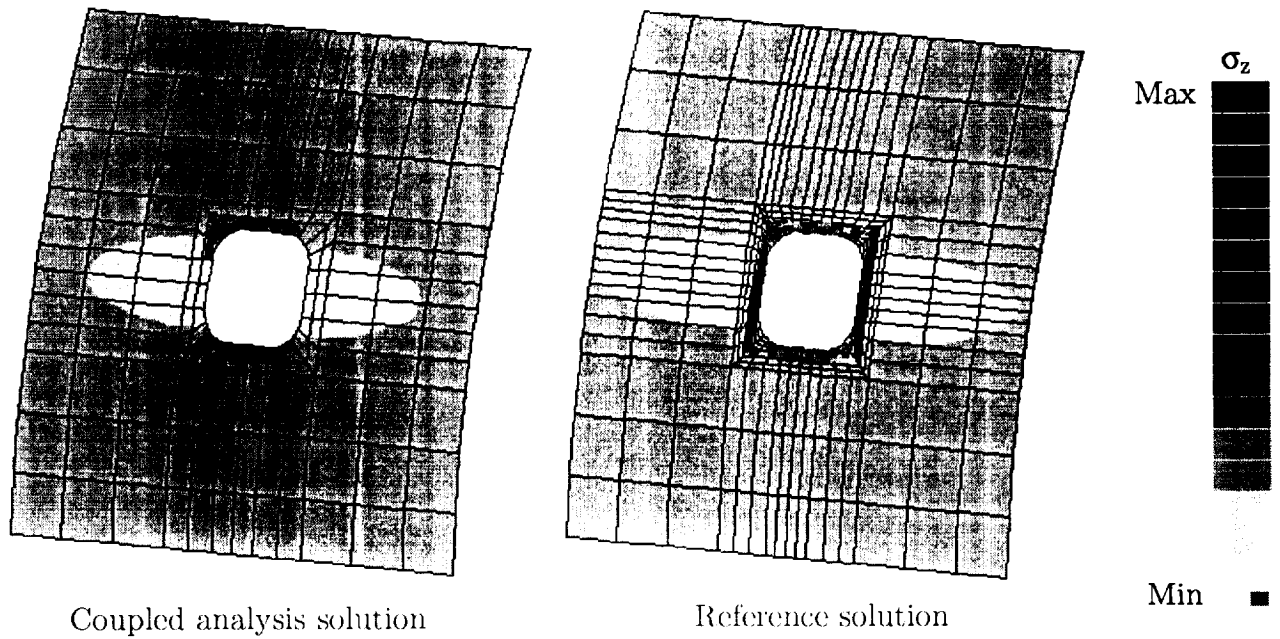
a. Global perspective

Coupled analysis solution   Reference solution

b. Local perspective

Figure 11. Deformed geometry

Coupled analysis solution   Reference solution

a. Global perspective

Coupled analysis solution   Reference solution
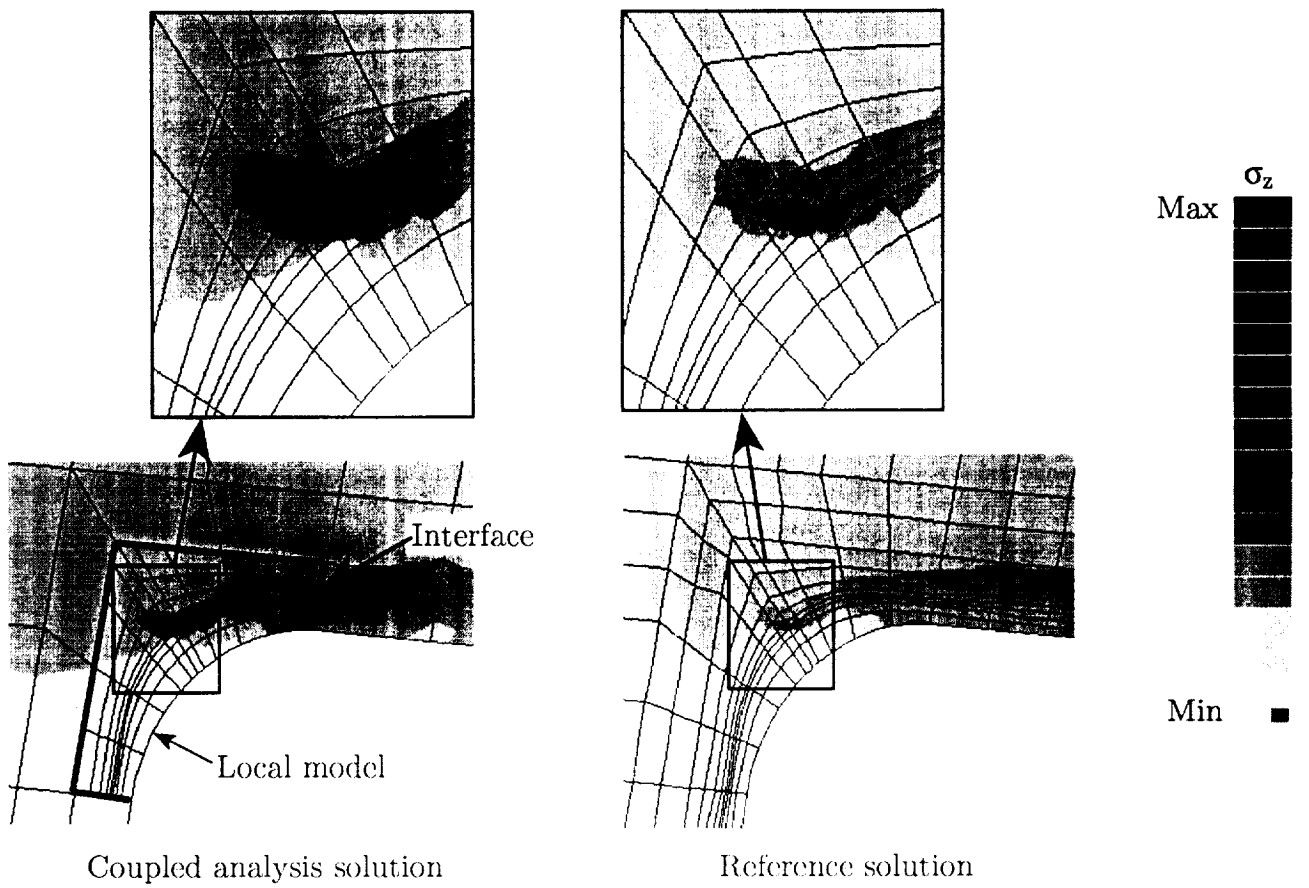
b. Local perspective

Figure 12. Axial stress, σ_z, distribution